BIOMECHANICAL VALIDATION OF A NEW BIOFIDELIC DUMMY

Schäuble, Andreas
DEKRA Automobil GmbH
Germany

Weyde, Michael
Büro für Unfallrekonstruktion Berlin
Germany

Paper Number 19-0197

ABSTRACT

In order to improve the preciseness in pedestrian-vehicle accident reconstructions, a new biofidelic dummy had been developed. The objective of this work was to biomechanically validate the biofidelity of this new kind of anthropomorphic testing device. Therefore, nine crash tests have been conducted with the biofidelic dummy and the results were compared with four crash tests earlier performed with the Žilina dummy, an anthropomorphic testing device widely used in accident research due to its low cost and robustness, cadaver tests obtained from published research papers and 21 real-world pedestrian accidents.

The trajectories of both anthropomorphic testing devices were computed and compared with those of cadaver tests, highlighting that the biofidelic dummy performs much more human-like than the Žilina dummy.

Damages to the vehicle's front caused by both anthropomorphic testing devices and real pedestrians were compared with each other, as realistic damages are very important for reconstruction purposes. It can be shown that the biofidelic dummy causes damages similar to those a pedestrian would cause in an accident of similar severity, whereas the Žilina dummy causes damages which are far too severe, which may mislead the expert witness to assume an impact velocity which is too slow.

The C-ratio, defined as closing speed over collision speed, was computed for both anthropomorphic testing devices, showing that the two deliver similar results. Computing the dynamic, time-dependent C-ratio, however, highlights differences in the kinematics and dynamics of the two anthropomorphic testing devices.

The throw distances of both anthropomorphic testing devices were compared with throw distance charts developed in-house by DEKRA based on experiments with the Žilina dummy and well-documented real-world accidents. The results show that the biofidelic dummy's behaviour is good.

Finally, the damages to the biofidelic dummy were analysed and transcribed to injuries of a human being. These "biofidelic dummy injuries" were compared with injuries of real pedestrians, focusing on five injuries, which can be used for reconstruction purposes. In general, the "injuries" of the biofdelic dummy correspond well with those of the pedestrian.

NOMENCLATURE

Acronyms

ADR	-	accident data recorder
ATD	-	anthropomorphic testing device
PMHS	-	post-mortem human subject

Symbols

C	-	ratio between closing speed and collision speed
$C(t)$	-	dynamic, time-dependent C-ratio
$C(t)_P$	-	dynamic, time-dependent C-ratio of the pelvis
$C(t; P)$	-	dynamic, time-dependent C-ratio relative to the pelvis
$C(t; P)_F$	-	dynamic, time-dependent C-ratio of the foot relative to the pelvis
$C(t; P)_H$	-	dynamic, time-dependent C-ratio of the head relative to the pelvis
CoM	-	centre of mass
e	-	coefficient of restitution

INTRODUCTION

While severe vehicle-vehicle accidents usually not only cause distinctive damages as well as scratch marks on the road surface, even lethal pedestrian-vehicle accidents often lead neither to significant traces on the road surface nor to a damage pattern which allows precise reconstruction of the vehicle's collision speed. This lack of evidence often complicates the work of experts reconstructing such kinds of accidents. Therefore, a need existed to improve the preciseness of accident reconstruction when pedestrians had been involved.

In order to achieve an improvement in accident reconstruction in this field, there seemed to be a need for a surrogate of an ATD, which was able to deliver realistic vehicle damages as well as damages on itself, which allow finding a correspondence between dummy damages and injury probability. As such, a team of students under the guidance of one of the others had developed a biofidelic dummy. This dummy was designed to cause realistic vehicle damages and furthermore to cause damages to itself comparable to typical injuries, which pedestrians sustain in a similar impact with a vehicle, in order to use the data gathered by conducting crash tests to reconstruct real pedestrian-vehicle accidents.

The objective of this research was to analyse and verify the biofidelity of this human surrogate in pedestrian-vehicle crash tests.

METHODS AND USED EQUIPMENT

DEKRA has conducted nine crash tests with the biofidelic dummy in conjunction with AXA Insurance in Wildhaus, Switzerland in the summer of 2018. The results have been compared with crash tests using the Žilina dummy, a dummy widely used in accident reconstruction due to its robustness and low price, and results of cadaver tests obtained from published research papers as well as 21 well-documented real-world pedestrian accidents. See table 1 for an overview of the crash tests.

The crash test videos have been analysed by the programme "Falcon" to obtain the dummy trajectories and the C-ratio. The frame rate of the videos is 500 pictures/s. Time is set to zero at the point of first contact between the dummy and vehicle, which is visualised by means of a light signal mounted on top of the vehicle. The coordinate system, which is required for the programme to make its calculations, has its origin at the first target on the vehicle. The *x*-direction faces in the direction of travel, while the *y*-direction faces upwards. The dummy targets, used by the programme to track the dummy movements, had to be applied manually to the dummy within the programme. Targets were applied to the head, hip and foot. Each body region was analysed three-times and the average value was calculated, in order to reduce any errors stemming from manually placing the targets on the dummy. Every 10^{th} picture has been analysed, i.e. the time interval between the different measurements is 0.02 s. "Falcon" provides "txt"-files as data output, which have been uploaded into "Excel", with which the lines have been drawn. The final trajectory graphs have been created with "CorelDraw".

"Autopsies" have also been performed on the biofidelic dummy, in order to obtain the damages the dummy sustained during the crash tests and to translate those damages to comparable injuries of a human being.

Table 1.
Overview of the crash tests

crash test	vehicle	collision speed	braking	dummy
wh18.22	BMW 1 Series 2004	75 km/h	pre-crash	biofidelic
wh18.23	BMW 1 Series 2004	99 km/h	in-crash	biofidelic
wh18.24	VW Touareg 2003	75 km/h	pre-crash	biofidelic
wh18.25	VW Touareg 2003	99 km/h	in-crash	biofidelic
wh18.26	VW Passat Variant 2006	75 km/h	pre-crash	biofidelic
wh18.27	VW Passat Variant 2006	99 km/h	in-crash	biofidelic
wh18.28	Mercedes A-Class 2005	72 km/h	pre-crash	biofidelic
wh18.29	Mercedes A-Class 2005	96 km/h	in-crash	biofidelic
wh18.34	VW Touareg 2003	27 km/h	in-crash	biofidelic
wh08.27	Ford Galaxy 1998	40 km/h	pre-crash	Žilina
wh08.28	BMW 523i 1998	40 km/h	pre-crash	Žilina
wh08.29	Toyota Avensis 1998	40 km/h	pre-crash	Žilina
wh10.12	Fiat Punto 1996	55 km/h	late or unbraked	Žilina

CRASH TEST DUMMIES USED IN ACCIDENT RECONSTRCUTION

Žilina dummy

The Žilina dummy was developed at the University of Žilina in the Slovak Republic, and represents a 50th percentile male.

In contrast to the more sophisticated ATDs used by the automotive industry, instrumentation is limited to the chest [1]. This ATD is based on a metal skeleton covered by hard plastic, and the joints can be fastened to enable an upright posture.

Biofidelic dummy

The first prototype had a wooden skeleton, which was held together by stapled straps, covered by a tissue surrogate made of a mixture of silicone and acrylic. The special feature of this ATD tissue are the pseudoelastic properties similar to human tissue. Under the application of an external force, the tissue behaves plastically, while its properties are elastic as soon as the force is removed. The skin was represented by a 3 mm thick wet suit, which is covered by latex to increase the elasticity and tensile strength. Moreover, the wet suit is not only used as a skin surrogate, but also as a means of additional fixation of the tissue parts.

In order to further improve the anthropometry and biofidelity of this 50th percentile male ATD, the current version has no longer wooden bones, but a mixture of epoxy resin and aluminium powder is used. This mixture allows for the fabrication of ATD bones, which better resemble human bones in their shape and mechanical properties. The tissue parts are now made of a two-component silicone instead of a mixture of silicone and acrylic. A wet suit, covered with latex, is still used as the skin surrogate.

RESULTS AND DISCUSSIONS

Dummy trajectories

The dummy trajectories were obtained for each crash test. However, the main characteristics are only explained based on one vehicle for each the biofidelic and Žilina dummy, as the differences between different vehicles are not that stark.

Biofidelic dummy Figure 1 displays the dummy trajectories of the crash tests wh18.22 and wh18.23. The "suck-below" effect, where the pedestrian's foot is sucked below the vehicle's front-end spoiler due to friction and inertia forces, becomes more accentuated with an increase in collision speed. This effect can induce large bending and shear forces close to the talocalcanean joint. The magnitude of this "suck-below" effect further influences the kinematics of the lower extremities. While the legs are catapulted higher into the air at the lower

collision speed, the lower extremities remain rather stuck to the vehicle's front due to the larger "suck-below" effect at the higher collision speed.

In the meantime, however, the ATD's torso is accelerated and moves along the vehicle's contour, leading to extensive stretching. Without the wet suit, the biofidelic dummy would most likely have been torn apart. The probability of dismemberment was analysed by [2]. They report a probability of dismemberment at a collision speed of 100 km/h of 0.281947 as mean, 0.157408 as lower and 0.514652 as upper value. The extensive stretching behaviour of the biofidelic dummy therefore does not seem to be unrealistic, but due to a lack of cadaveric tests at such high collision speeds it is difficult to assess the exact biofidelity of that behaviour.

In crash test wh18.22, the ATD's thigh is pushing backwards the left headlight assembly. This creates a sharp edge at the front part of the left fender. As the biofidelic dummy continues to slide onto the bonnet, this sharp edge pierces the ATD's leg. Such injuries are known from real-world accidents.

The head ultimately still impacts the windscreen at 70 km/h, while the head impacts the roof leading edge at 100 km/h. Hence, the head moves further along the vehicle's contour with an increase in collision speed.

The hip is also further elevated at the higher collision speed, partially due to the extensive stretching behaviour of the biofidelic dummy.

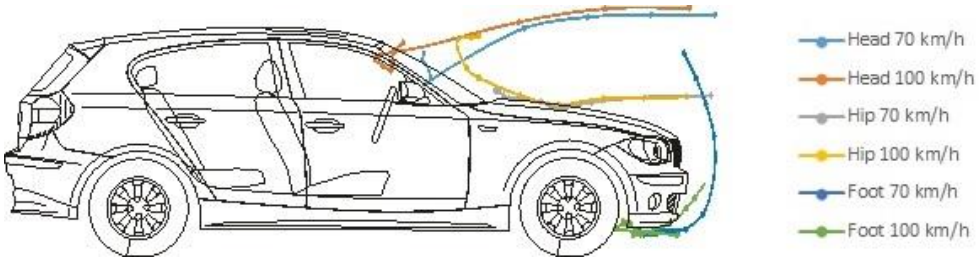

Figure 1. Dummy trajectories of crash tests wh18.22 and wh18.23.

Žilina dummy Figure 2 displays the dummy trajectories of crash test wh08.27.
Here, the "suck-below" effect is much less pronounced. This has two reasons. Firstly, the collision speed of 40 km/h is much lower than the collision speeds of 70 km/h and 100 km/h used with the biofidelic dummy, meaning that the effect is automatically less accentuated. Secondly, the Žilina dummy is made of steel. Thus, the ATD's bones bend less than those of the biofidelic dummy and can further not huddle against the vehicle's contour in the same way as the latter's one. The lower extremities are immediately catapulted away from the vehicle and the ATD rotates onto the bonnet around its *CoM*.

The legs' collision with the bumper is elastic. A speed for the measured leg of 44.87 km/h was recorded 0.02 s after impact. Considering that the collision speed was 40 km/h, this leads to a coefficient of restitution of e=1.12. Normally, however, $e \leq 1$, but the determination of the ATD's velocity by means of the programme "Falcon" is afflicted with minor errors. Thus, it can be concluded that the collision is perfectly elastic. Human tissue, however, is pseudoelastic. The tissue surrogate of the biofidelic dummy therefore exhibits pseudoelastic properties. In crash test wh18.22, the determined coefficient of restitution is e=0.63. This explains why the legs of the biofidelic dummy huddle against the vehicle's contour. The impact force causes the dummy tissue to deform and the impact energy is absorbed due to this plastic behaviour, which means that less energy is available for the legs to be catapulted away.

As the torso of the Žilina dummy rolls onto the bonnet, the ATD props itself on its arm, before the head subsequently impacts the windscreen. The rotation around the *CoM* continues.

In general, the ATD remains stiff throughout the whole impact and there is no stretching behaviour as compared with the biofidelic dummy.

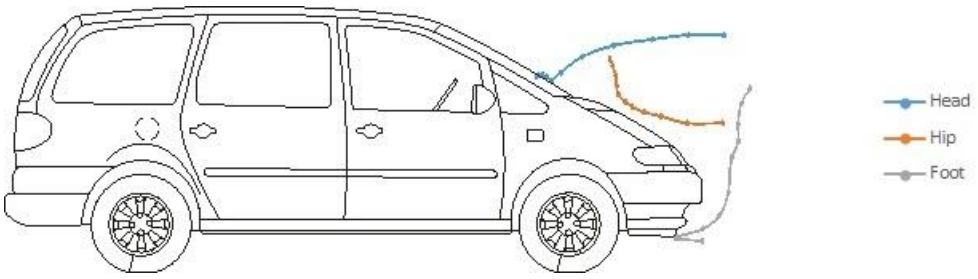

Figure 2. Dummy trajectories of crash test wh08.27.

Comparison with PMHS-tests In order to validate the biofidelity of the trajectories of both the biofidelic and Žilina dummy, the findings were compared with PMHS-tests published in research papers.

[3] conducted four PMHS-tests. They used a mid-sized sedan and a small city car, and the collision speed was 40 km/h. The four cadavers were male and exhibited no pre-existing fractures, lesions or other bone pathology, though three of the subjects had poor bone mineral density.

Figure 3 displays the trajectories of the PMHS-tests using the mid-sized sedan, the biofidelic dummy tests with the VW Passat, and the Žilina dummy test with the Toyota Avensis. The VW Passat and the Toyota Avensis were chosen for comparison as they should equal the mid-sized sedan in weight the most and should also have a similar front-end geometry. However, the different collision speeds must be taken into account, making a direct comparison somewhat complicated.

The PMHSs exhibit the "suck-below" effect similar to the ATDs, before the lower extremities rebound and swing upwards. The trajectories of the PMHSs' lower extremities resemble a circle, while the Žilina dummy's foot swings upwards much steeper. The trajectory of the biofidelic dummy's foot resembles rather the PMHSs, though the lower extremities slide off the front-end in course of the impact, which makes a direct comparison somewhat difficult. Considering the head and hip, no stark contrasts can be determined between the PMHSs and ATDs. The only major difference is that the Žilina dummy's head did not impact the bonnet/windscreen, as the dummy propped itself on its arm.

[3] further computed the body part trajectories relative to the pelvis as shown in figure 4. Figure 5 depicts the dummy trajectories relative to the pelvis of the biofidelic and Žilina dummy. The trajectories of the heads of both ATDs form a cloud and there are no major differences between the individual trajectories, even though the collision speeds are quite different between the biofidelic and Žilina dummy. Considering the feet of the two ATDs, however, two different clusters are formed. The feet of the Žilina dummies swing upwards much faster, also inducing a faster hip rotation, while the feet of the biofidelic dummies swing upwards much slower. At the beginning, these trajectories are also pretty vertical, which is explained first by the "suck-below" effect, second by the huddling of the lower extremities against the front-end structure and third by the stretching of the lower extremities.

Thus, there are hardly any differences in the head trajectories relative to the pelvis between the biofidelic and Žilina dummy. However, the upper body kinematics are still different. Regarding the lower extremities, though, there are stark differences. These are primarily explained by the fact that the biofidelic dummy is a pseudoelastic body, while the Žilina dummy is an elastic body.

Comparing the trajectories of the ATDs with the PMHSs, bearing in mind that the collision speeds differ, the trajectories of the biofidelic dummy match those of the PMHSs more than the Žilina dummy does. The lower extremities of the PMHSs swing upwards in a slower fashion just as the biofidelic dummy does, being explained by a prolonged contact phase between the PMHS's lower extremities and the vehicle's front-end compared to the Žilina dummy, as the human body is a pseudoelastic body as well.

[4] conducted three PMHS-tests at 40 km/h with a small sedan. Figure 6 shows the crash sequence of one of these tests compared with one biofidelic dummy test and Žilina dummy test. These two ATD tests have been chosen for comparison purposes due to the same reasons as above. While the Toyota Avensis has the same collision speed of 40 km/h as the PMHS-test, it is stressed again that the collision speed of the VW Passat is much higher at 75 km/h. The different kinematics of the Žilina dummy can be easily noted, especially the fact that the chest props

itself on the arm and thereby lifts the waist off the bonnet. The biofidelic dummy, on the other hand, huddles against the vehicle's contour.

Thus, it can be concluded that the trajectories of the biofidelic dummy are much more human-like than those of the Žilina dummy. In particular, the "propping" effect of the latter is unnatural. These findings come, however, with the caveat that the collision speeds are quite different. Nonetheless, the tendency that the biofidelic dummy behaves more humanoid cannot be dismissed.

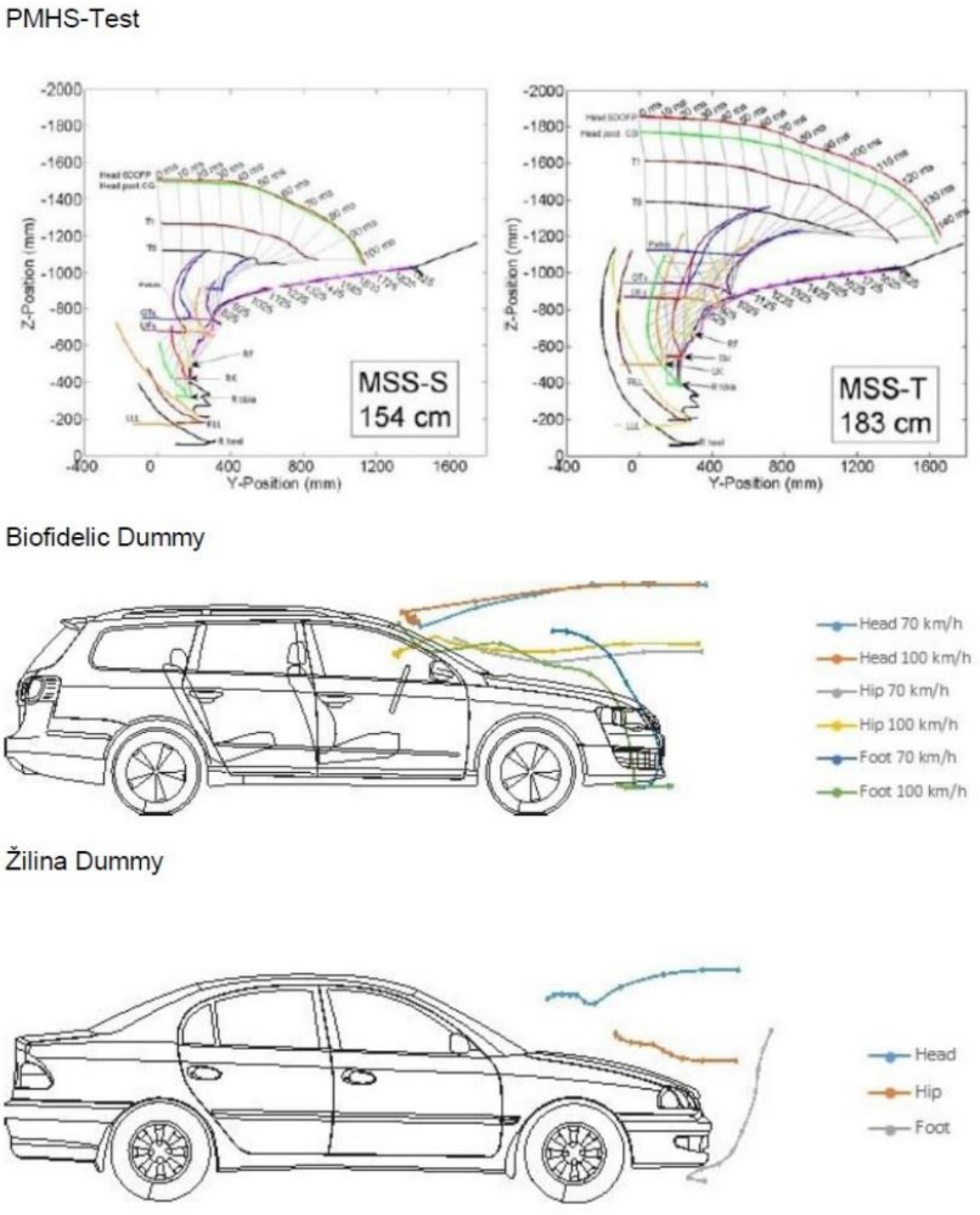

Figure 3. Comparison between trajectories of PMHS, biofidelic dummy and Žilina dummy. Top: MSS-S: mid-sized sedan small subject (body height); MSS-T: mid-sized sedan tall subject (body height) [3]. Middle: crash tests wh18.26 and wh18.27. Bottom: crash test wh08.29.

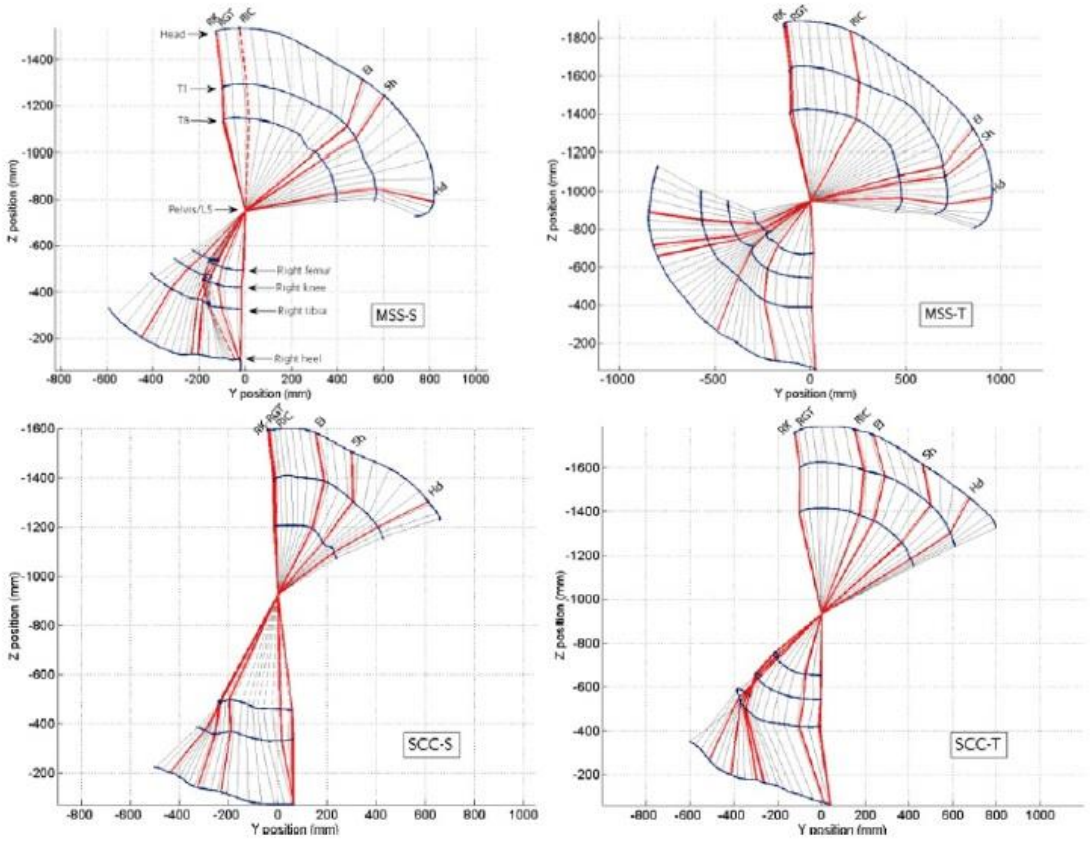

Figure 4. PMHS trajectories relative to the pelvis. MSS-S: mid-sized sedan small subject; MSS-T: mid-sized sedan tall subject; SCC-S: small city car small subject; SCC-T: small city car tall subject [3].

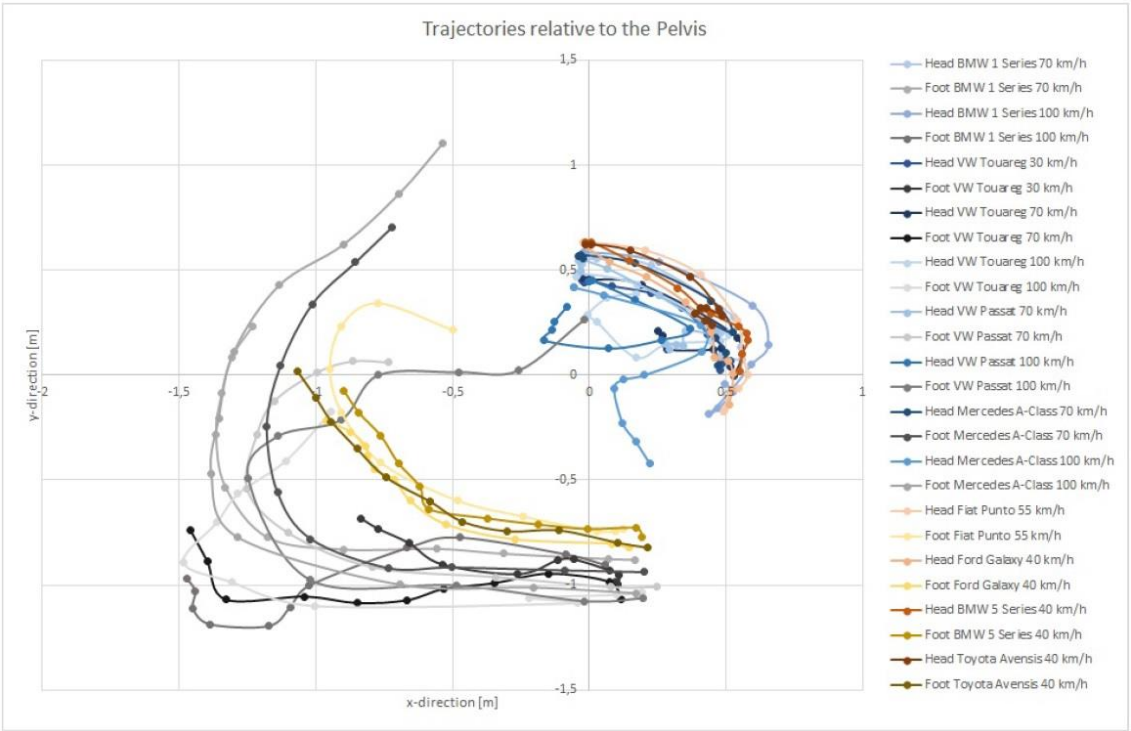

Figure 5. ATD trajectories relative to the pelvis. Blue: biofidelic dummy's head; Grey: biofidelic dummy's foot; Orange: Žilina dummy's head; Gold: Žilina dummy's foot.

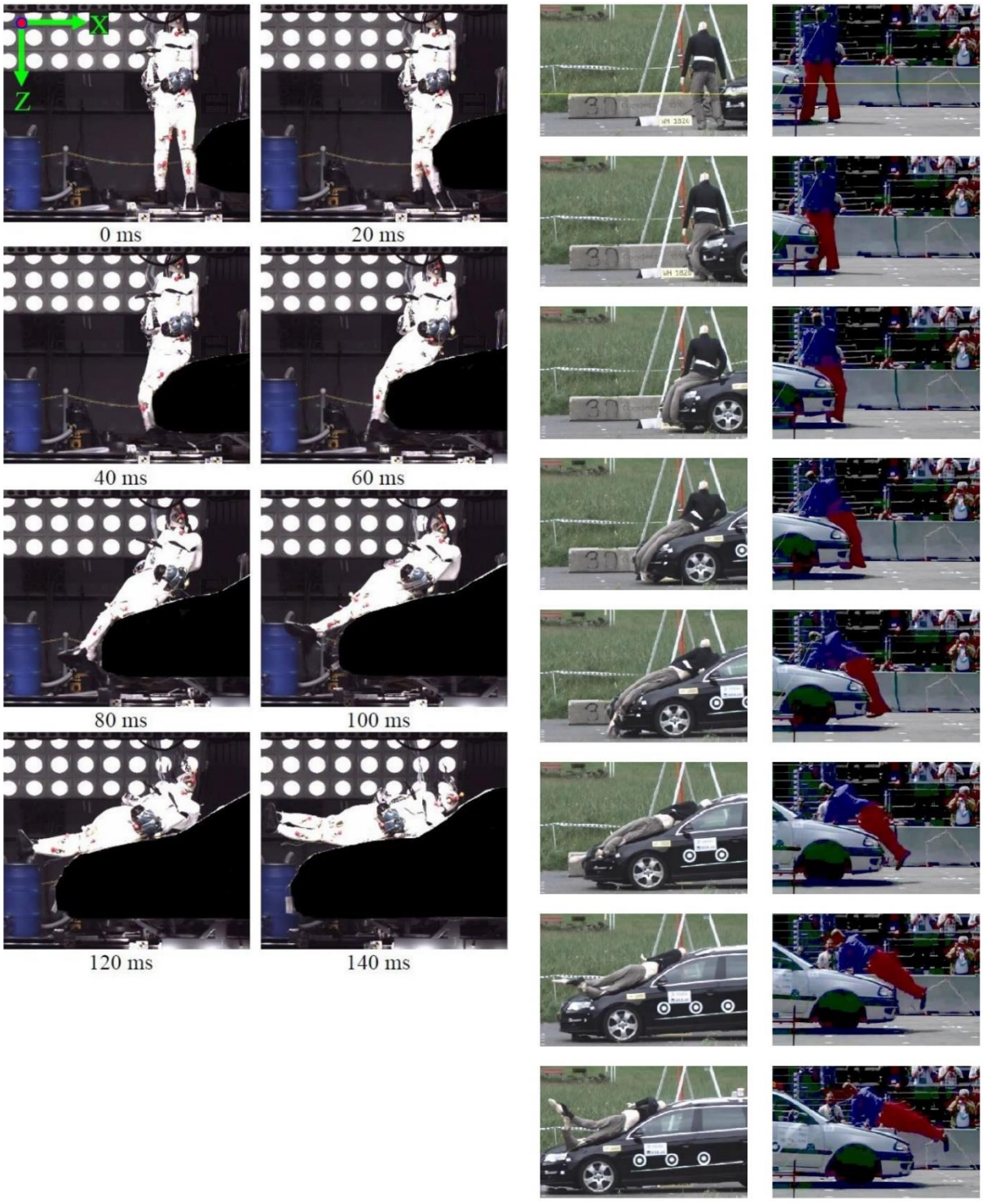

Figure 6. Crash sequences of a PMHS (left) [4], biofidelic dummy (middle) and Žilina dummy test (right) at 20 ms intervals.

Vehicle Damages
For reconstruction purposes, it is very important that the vehicle damages caused by the ATD are comparable to those caused by the pedestrian. Of the nine crash tests with the biofidelic dummy, only crash tests wh18.22 and wh18.26 are comparable to two of the analysed real-world accidents. The collision speed, dummy/pedestrian height and weight are still within an acceptable deviation.

Considering the Žilina dummy, all four crash tests are considered, even though the collision speed is much lower.

Next to the different collisions speeds and differences in dummy and pedestrian anthropometry, differences in front-end geometry and local vehicle stiffness should also be born in mind.

Biofidelic dummy vs. pedestrian The damages to the bonnet leading edge caused by both the biofidelic dummy and the two pedestrians are shown in figure 7.

Figure 7. Vehicle damages biofidelic dummy vs. pedestrian. Top Left: wh18.22; Bottom left: wh18.26; Top right: accident 1: Bottom right: accident 2.

In both accidents, the thigh and hip rolled over the bonnet leading edge and onto the bonnet causing the damages as seen in figure 7. The bonnets are slightly indented and the headlight assembly of the BMW is pushed backwards.

Considering the two crash tests, the damages were also caused by the thigh and hip. As in the real-world accidents, the bonnets are slightly indented and the headlight assembly of the BMW is pushed backwards too with the glass being fractured.

The damages produced by the biofidelic dummy match those caused by the two pedestrians pretty well.

Žilina dummy vs. pedestrian The damages to the bonnet leading edge caused by both the Žilina dummy and the two pedestrians are shown in figure 8.

Even though the collision speed is much lower in the crash tests, the damages are much more intense. The thigh and hip of the Žilina dummy indented the bonnet leading edge much further than the two pedestrians did. Moreover, the bonnet is bulged by this impact, before the chest of the ATD indents it much deeper than the pedestrians did. The pattern of the damages is completely different and cannot be compared with the two real-world accidents.

As the Žilina dummy is a rigid body, it can also cause scratch marks on the bonnet or even lacerate metal parts of the vehicle. A human being cannot cause such damages.

The Žilina dummy causes damages that are much more intense even at a lower collision speed. Hence, it can be concluded that the Žilina dummy does not produce realistic damages and would suggest a lower collision speed when compared with a similar real-world accident.

Figure 8. Vehicle damages Žilina dummy vs. pedestrian. Top left: wh08.27; Upper left: wh08.28; Lower left: wh08.29; Bottom left: wh10.12; Top right: accident 1; Bottom right: accident 2.

C-ratio

The C-ratio is defined as the closing speed over collision speed, and is an important parameter in accident reconstruction.

In practice, the C-ratio is determined using the pedestrian's anthropometric data and the vehicle's geometry. This geometrical C-ratio is determined using an internal DEKRA programme.

Here, it shall be analysed in how far the ATD's C-ratio determined using the geometrical approach matches the one determined by using crash test video analysis. The C-ratio is determined by evaluating the *CoM*'s speed at just that moment when the whole ATD detaches from the vehicle. Table 2 lists the determined C-ratios.

Table2.
C-ratios (the smallest deviation is marked in red)

crashtest	C	geometrical C	geometrical C 5%	geometrical C 10%	geometrical C 15%	ΔC	ΔC 5%	ΔC 10%	ΔC 15%	ΔC%	ΔC% 5%	ΔC% 10%	ΔC% 15%
wh18.22	90	74	78	82	86	-16	-12	-8	-4	-17,78	-13,33	-8,89	-4,44
wh18.23	100	72	76	80	84	-28	-24	-20	-16	-28,00	-24,00	-20,00	-16,00
wh18.24	95	87	91	95	99	-8	-4	0	4	-8,42	-4,21	0,00	4,21
wh18.25	80	86	90	94	98	6	10	14	18	7,50	12,50	17,50	22,50
wh18.26	97	73	77	81	85	-24	-20	-16	-12	-24,74	-20,62	-16,49	-12,37
wh18.27	100	73	77	81	85	-27	-23	-19	-15	-27,00	-23,00	-19,00	-15,00
wh18.28	77	72	76	80	84	-5	-1	3	7	-6,49	-1,30	3,90	9,09
wh18.29	93	71	75	79	83	-22	-18	-14	-10	-23,65	-19,35	-15,05	-10,75
wh18.34	87	87	91	95	99	0	4	8	12	0,00	4,60	9,19	13,79
sum										**15,95**	**13,66**	**12,22**	**12,02**
wh10.12	90	72	76	80	84	-18	-14	-10	-6	-20,00	-15,56	-11,11	-6,67
wh08.27	102	79	83	87	91	-23	-19	-15	-11	-22,55	-18,63	-14,71	-10,78
wh08.28	70	68	72	76	80	-2	2	6	10	-2,86	2,86	8,57	14,29
wh08.29	66	72	76	80	84	6	10	14	18	9,09	15,15	21,21	27,27
sum										**13,63**	**13,05**	**13,90**	**14,75**

C is the C-ratio determined by means of video analysis and is the reference value. Depending on the impact characteristics, a correction factor of between 5% and 15% is applied to the geometrical C-ratio. This is marked as "geometrical *C* 5%", for example. The difference between the two C-ratio values is marked with Δ*C*, while the percentage-wise difference with Δ*C*%. A "minus" indicates that the value is less than the reference value.

While the deviation in sum decreases with an increase of the correction factor for the biofidelic dummy, the deviations are more or less the same for the Žilina dummy, though the correction factor of 5% exhibits the smallest deviation. The respective deviation is sum with no correction factor and a 5% correction factor for the biofidelic dummy is higher compared to the Žilina dummy, while the deviation in sum is lower for the biofidelic dummy compared to the Žilina dummy with a correction factor of 10% and 15%, respectively.

Regarding the biofidelic dummy, positive deviations only occur in crash tests conducted with the VW Touareg and Mercedes A-Class. Looking at the Žilina dummy, positive deviations occur in the crash tests with the BMW 5 Series and the Toyota Avensis.

Considering the biofidelic dummy, Δ*C*% ~25 for all the cases where the ATD hit the roof leading edge and remained attached to it for at least a short time. In crash test wh18.28, the ATD impacted the roof leading edge, but detached immediately. As the different correction factors are applied, the values for Δ*C*% all decrease in a similar pattern.

How different front-end geometries and the fact that the roof leading edge has been impacted affect this behaviour merits further investigation.

Dynamic, time-dependent C-ratio While the C-ratio is a single value determined at the point of ATD detachment, the dynamic, time-dependent C-ratio, *C(t)*, is the fraction between closing speed and collision speed at any point of time. It visualises how the ATD/pedestrian gains energy, and hence speed, during the primary impact, and how the impact energy is then slowly absorbed during the secondary and tertiary impacts. Figures 9, 10 and 11 show the dynamic, time-dependent C-ratio for the head, hip and foot, respectively.

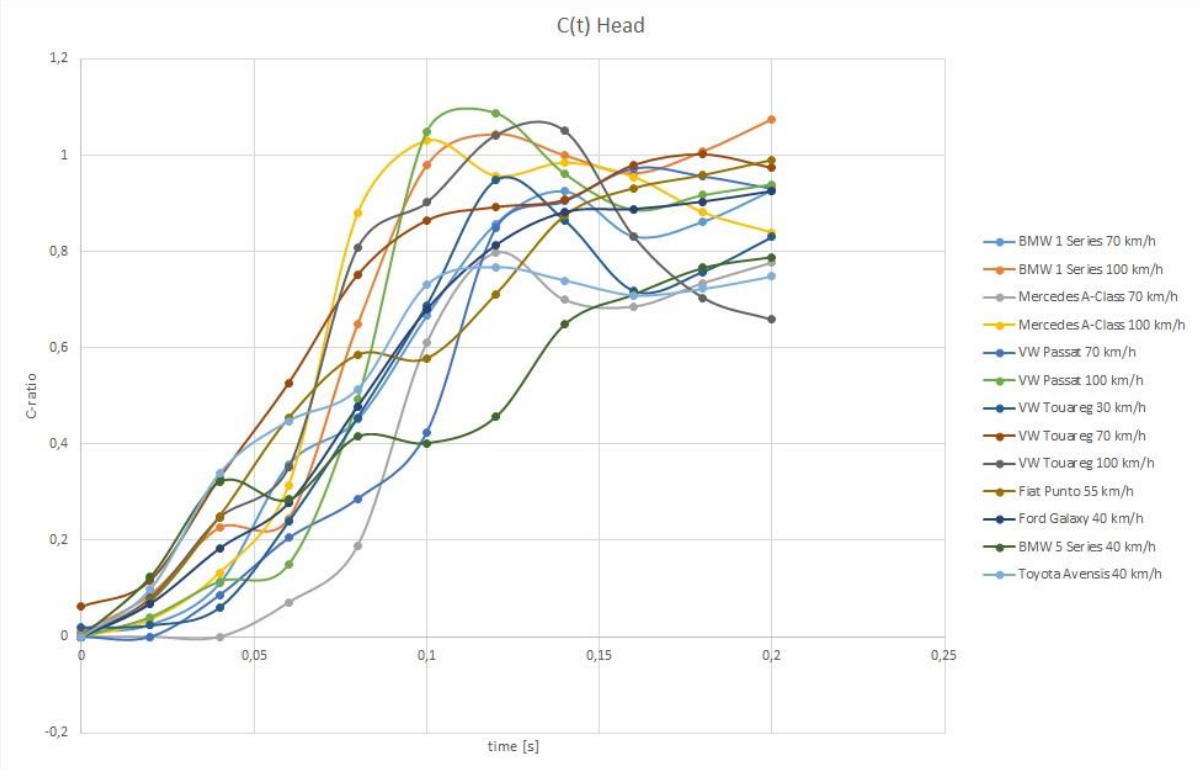

Figure 9. C(t) of the head.

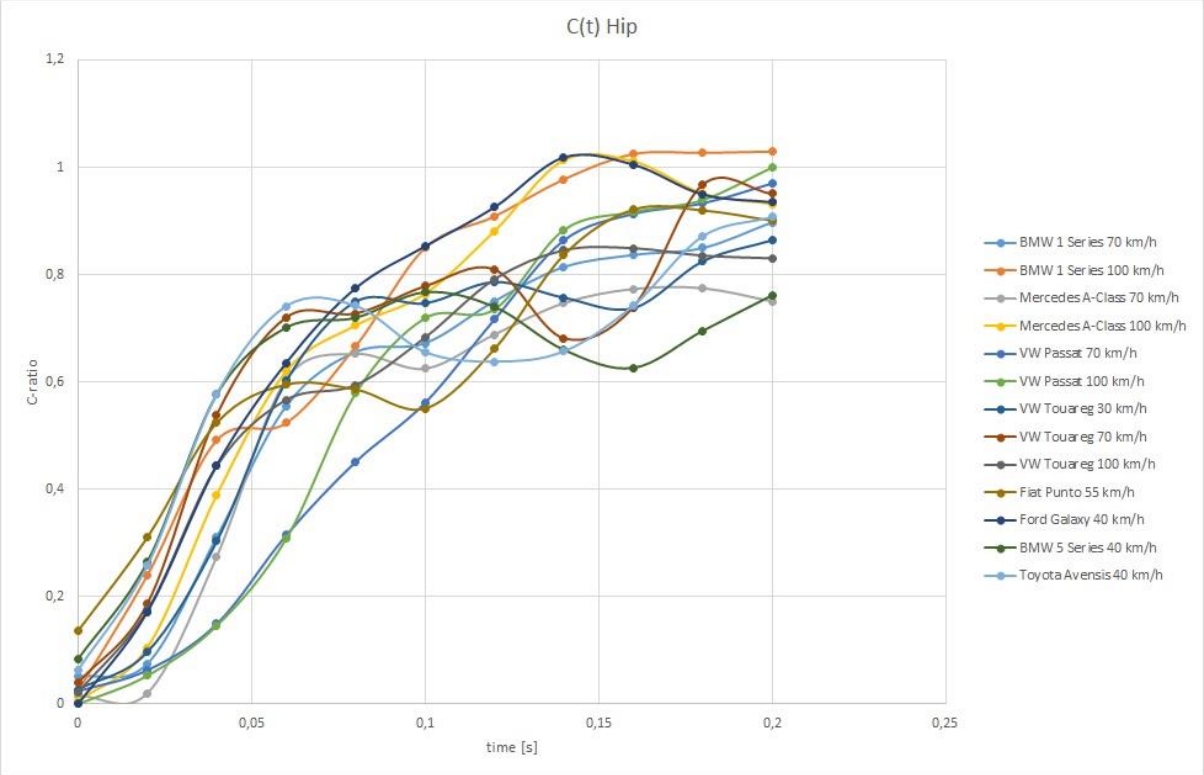

Figure 10. C(t) of the hip.

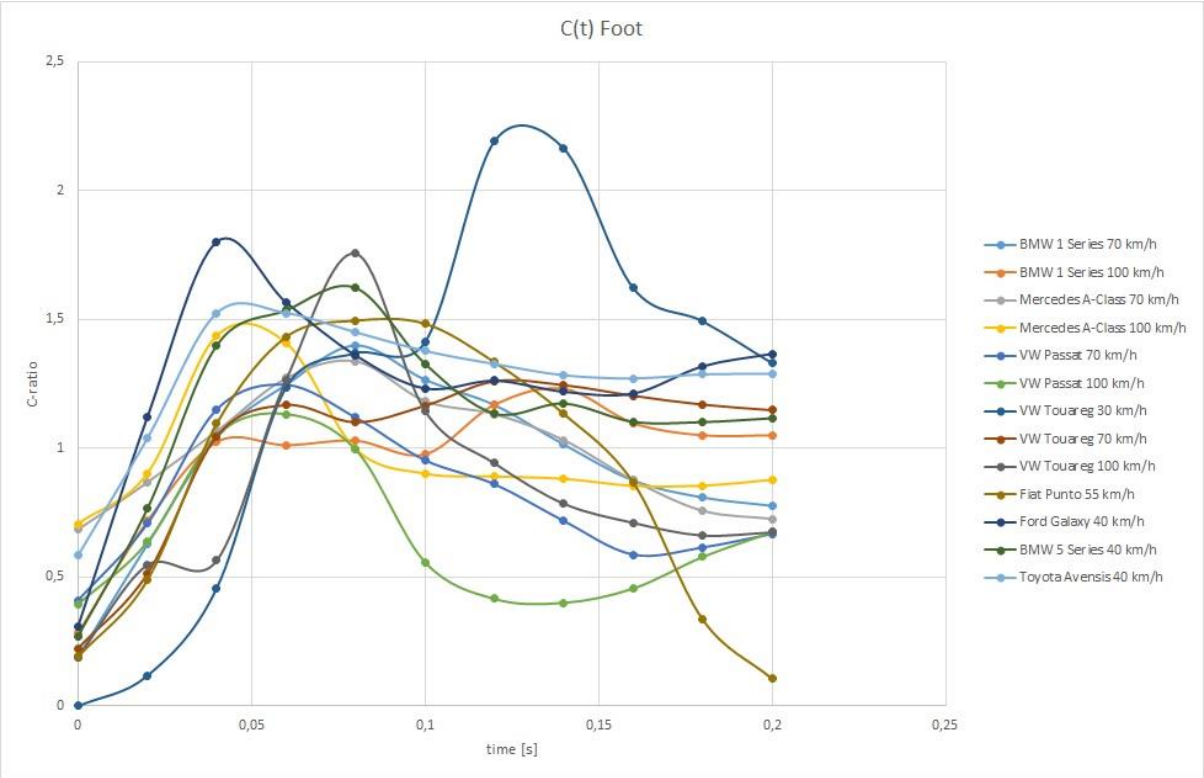

Figure 11. C(t) of the foot.

Considering the head and hip of the biofidelic dummy, certain patterns can be spotted, while the response of the foot seems to strongly depend on the specific front-end geometry and the subsequent dynamics and kinematics of the ATD. Especially the magnitude of the "suck-below" effect seems to influence the behaviour, as well as whether the leg is pierced by any sharp edges such as in crash tests wh18.22 and wh18.26. The shapes of the "head-curves" and "hip-curves" are oftentimes relatively similar for the different collision speeds when impacted by the same vehicle. With an increase in collision speed, they only shift more towards the left and upwards as shown in figure 12.

Figure 12. C(t) of the head when hit by the BMW 1 Series (biofidelic dummy).

Considering the same body part, e.g. the head, at the same collision speed, the shapes of the curves are relatively similar, though the different front-end geometries do have an influence on *C(t)* as shown in figure 13.

In comparison to the biofidelic dummy, the different curves have unsurprisingly a much steeper slope for the Žilina dummy. As the Žilina dummy is an elastic body, less energy is absorbed by the impact itself, and hence the ATD gains more energy compared to the biofidelic dummy, resulting in a steeper increase in speed, especially regarding the lower extremities. However, similar to the biofidelic dummy, there seems to be no recognisable pattern for the lower extremities. For the head and hip, the shape of the curves is relatively similar to each other at the same impact speed with some influence of the front-end geometry as shown in figure 14. Note, however, that the Fiat Punto has a slightly higher collision speed.

Dynamic, time-dependent C-ratio relative to the pelvis As with the dummy trajectories relative to the pelvis, the dynamic, time-dependent C-ratio, *C(t)*, of the head and foot can also be analysed relative to the pelvis.

Plotting *C(t; P)* over time, it can be seen that the heads of both the biofidelic and Žilina dummy behave in similar ways, while there is hardly any pattern discernable considering the feet (see figure 15). The shape of the head's *C(t; P)*-graph resembles more or less a sine curve with decreasing amplitude. The only exception constitutes crash test wh18.34, i.e. a biofidelic dummy being hit by a VW Touareg at 30 km/h.

Figure 16 depicts *C(t; P)* plotted over distance. Here, a much more distinct pattern can be discerned considering the heads and feet measured relative to the pelvis.

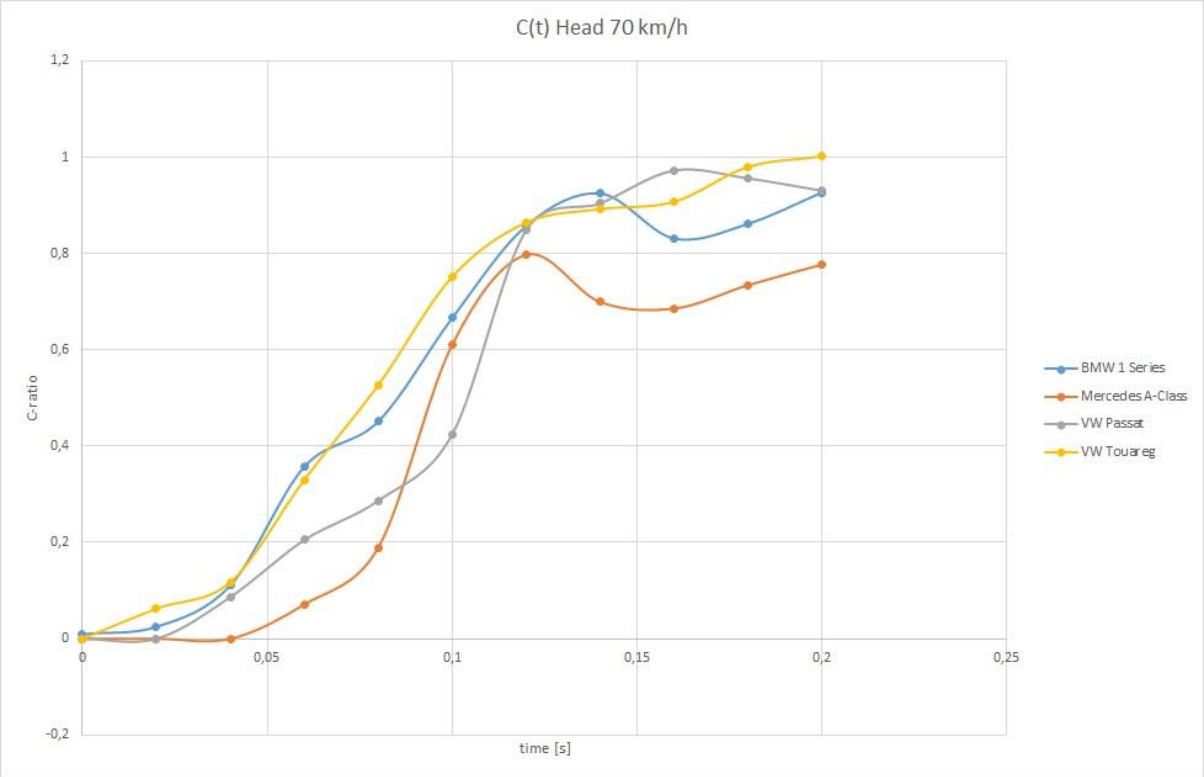

Figure 13. C(t) of the head at 70 km/h (biofidelic dummy).

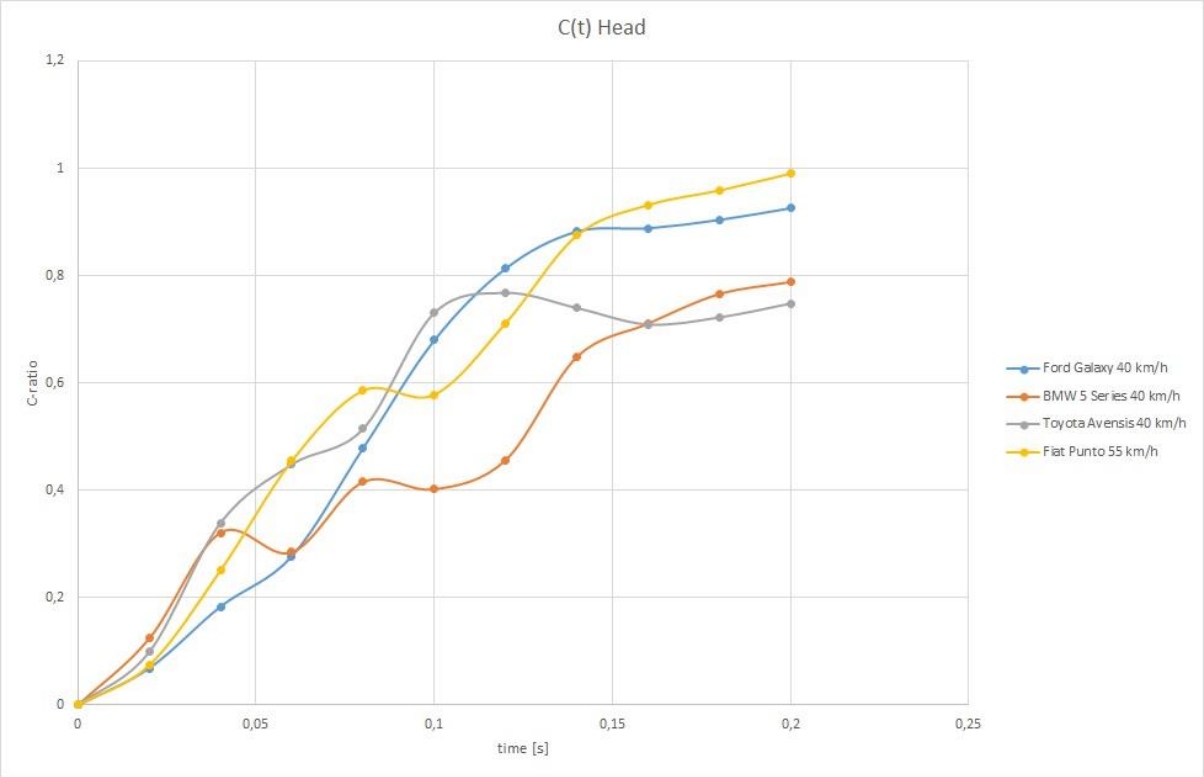

Figure 14. C(t) of the head (Žilina dummy).

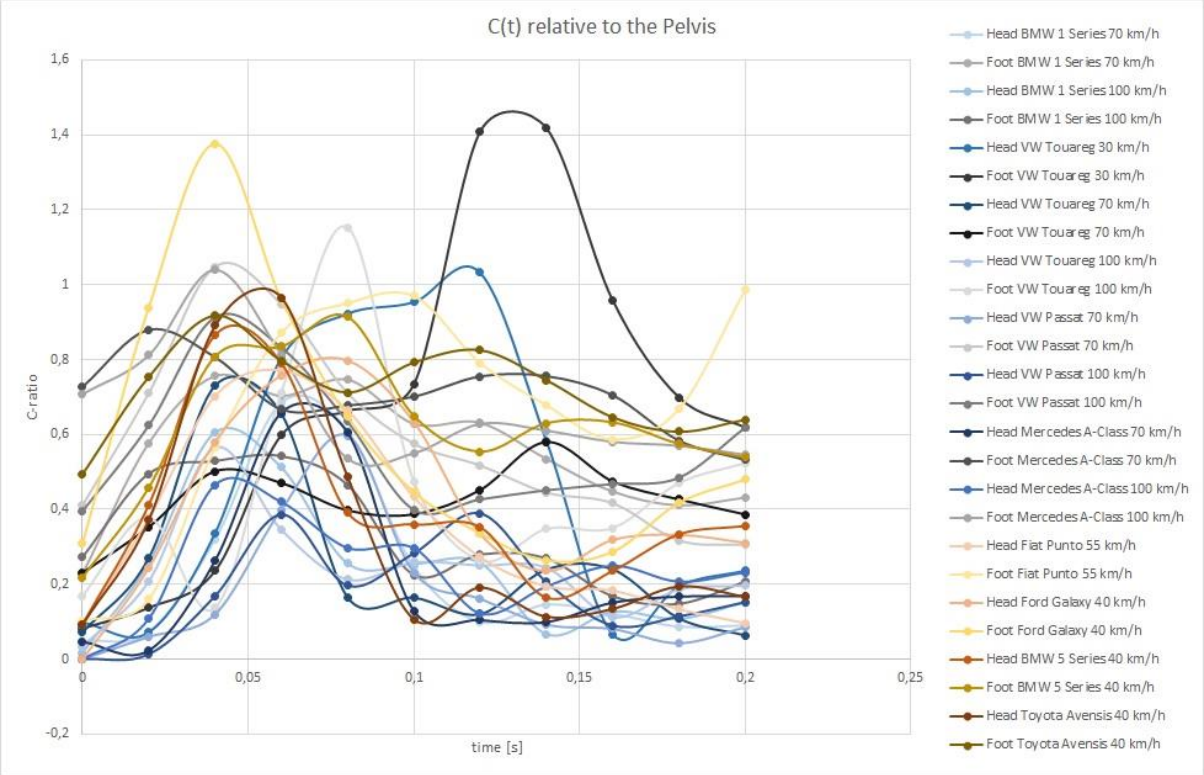

Figure 15. C(t) relative to the pelvis plotted over time. Blue: biofidelic dummy's head; Grey: biofidelic dummy's foot; Orange: Žilina dummy's head; Gold: Žilina dummy's foot.

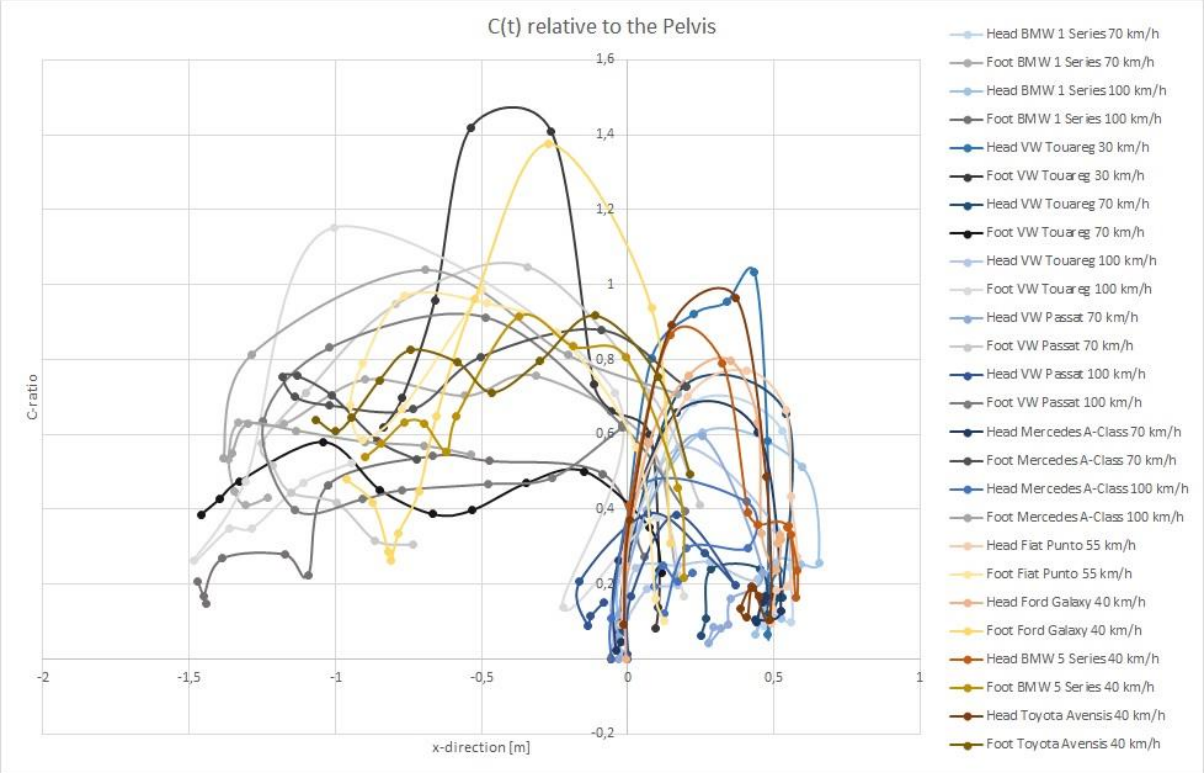

Figure 16. C(t) relative to the pelvis plotted over distance. Blue: biofidelic dummy's head; Grey: biofidelic dummy's foot; Orange: Žilina dummy's head; Gold: Žilina dummy's foot.

First, this graph visualises the kinematics and dynamics of the ATDs, which the first one does not. It is shown that, relative to the pelvis, the head is accelerated towards the striking vehicle, while the lower extremities are accelerated away from the vehicle. However, the behaviour of the different heads is very similar. The graphs resemble a negative square parabola, i.e. the head first experiences a positive acceleration relative to the pelvis and then a negative one. As *C(t; P)* is a ratio, one can argue that the heads experience a similar relative acceleration irrespective of collision speed and front-end geometry. On the other hand, the behaviour of the feet does not allow for any discernable patterns. Neither the biofidelic nor the Žilina dummy exhibit a distinct pattern, nor are there any particular characteristics concerning the collision speed or front-end geometry. The dynamic, time-dependent C-ratio of the foot relative to the pelvis seems to exhibit a completely random behaviour.

From this analysis, it can be concluded that the first collision between the striking vehicle and the pelvis is the primary determining factor considering the dynamics and kinematics of the ATD, and hence most possibly the pedestrian. As the heads exhibited more or less the same relative accelerations, the impact of the pelvis may thus have a direct influence on the injury mechanism and severity of the injuries to the head/neck complex. As the graphs resemble a negative square parabola and thus first exhibit a positive slope followed by a negative slope, the head first experiences an acceleration relative to the pelvis which is followed by a deceleration. As $C(t; P)_H$ is dependent on the pelvis, one can deduce that if $C(t)_P$ increases, $C(t; P)_H$ will increase too, i.e. the head will impact at a higher speed. Consequently, by reducing $C(t)_P$, the severity of head injuries may be reduced. As the head and pelvis are "connected" by the chest, the severity of chest injuries may possibly be lowered, too. $C(t)_P$, and thus $C(t; P)_H$, may be lowered by increasing the detaching time, i.e. allowing for greater deformation at the site of pelvis impact. Therefore, the local vehicle stiffness around the bonnet leading edge may be a decisive factor influencing both the kinematics and dynamics, as well as the injury mechanisms and injury likelihood of the upper body.

The influence of the pelvis on the head is much greater than on the lower extremities. Considering the latter, the magnitude of the "suck-below" effect and the height of the bonnet leading edge may have a decisive influence. While the front-end geometry seems to have a minor effect on the behaviour of the head relative to the pelvis, the influence on the lower extremities relative to the pelvis is much greater. The variability of $C(t; P)_F$ may also be explained by the anatomy of human beings. While the head and pelvis are "connected" to each other via the rather rigid spinal column, the feet and pelvis are "connected" to each other via the legs, which allow for greater relative movements.

[3] already concluded by means of PMHS-tests that the motion of the pelvis has an effect on the kinematics of both the upper body and lower extremities. These findings warrant further investigation.

Throw distance

Given that both the final position of the pedestrian as well as the point of collision are known, the throw distance can be used to determine the collision speed.

Throw distance charts have been developed by DEKRA based on crash tests with the Žilina dummy and results from well-documented real-world pedestrian accidents. Different throw charts have been developed for complete, partial and streaking hits. Considering complete hits, one has to further distinguish between pre-crash and in-crash braking.

Regarding the four pre-crash braking crash tests with the biofidelic dummy, two of the throw distances lie within the boundaries, while one lies just above the upper boundary and the fourth throw distance lies outside of the empirically developed corridor. However, DEKRA accident analysts deemed the deviation still being within an acceptable range. The three pre-crash braking crash tests with the Žilina dummy are also marked in the chart. Two of the three distances lie just below the lower boundary, while one lies outside the corridor. As the deviation is unacceptably high, data from the ADR have been analysed. The data highlight the fact that the brakes were not applied with full force, and hence the ATD was not catapulted away from the vehicle, but "travelled" with the vehicle for a prolonged time. This falsified the throw distance, which is why the Ford Galaxy must be excluded. Figure 17 shows the throw distance chart for complete hits and pre-crash braking.

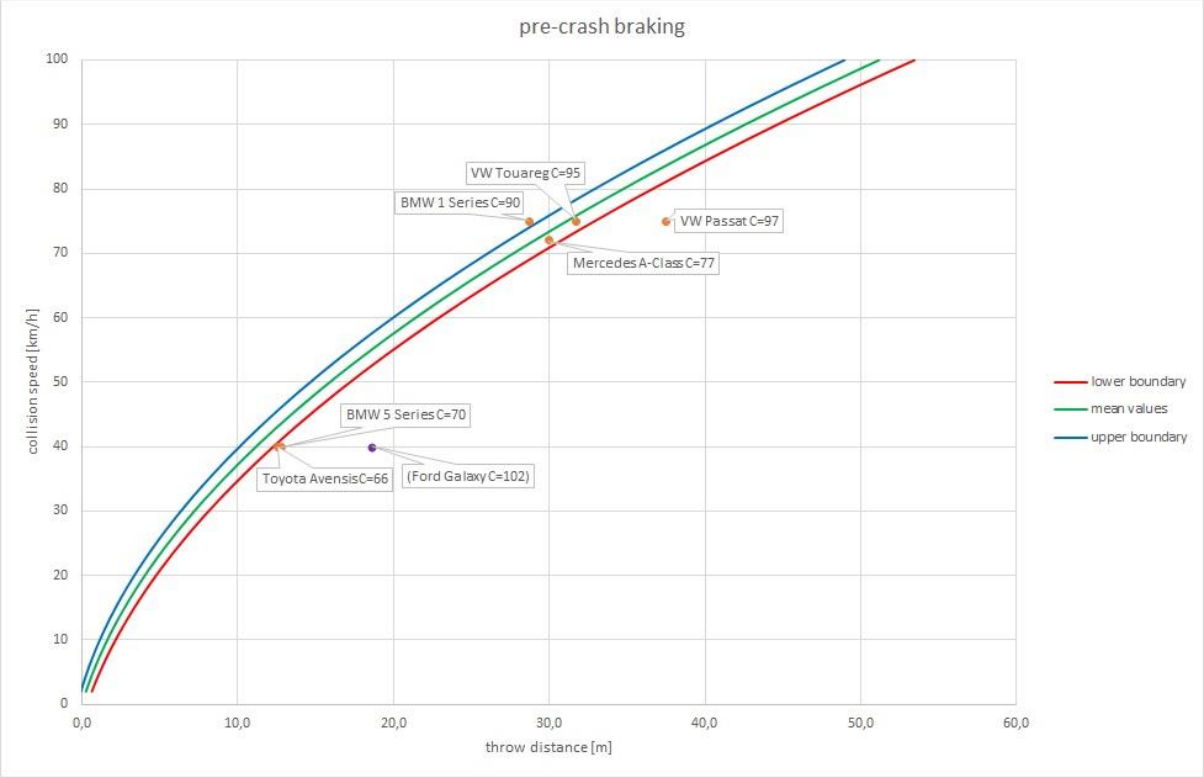

Figure 17. Throw distance chart for complete hits and pre-crash braking.

Considering in-crash braking, only three of the four crash tests conducted with the biofidelic dummy can be analysed. In crash test wh18.27, the ATD penetrated the windscreen and got stuck. While the throw distance for the Mercedes A-Class lies within the boundaries, the throw distance for the BMW 1 Series lies outside the boundaries, but still within an acceptable range according to DEKRA accident analysts. Regarding the VW Touareg, however, the deviation is by far too big. But, by further analysing the dynamics and kinematics of the ATD in this crash test, one realises that the ATD begins to slide off the fender quite immediately after impact and the complete hit hence becomes a partial hit. The throw distance lies well within the boundaries for partial hits. Thus, crash test wh18.25 is a special case, as the impact constellation equals to a complete hit, but turns into a partial hit due to the ATD kinematics and dynamics. This is explained by the flexibility of the biofidelic dummy. Like a human, the biofidelic dummy allows for torsional movement of the upper body relative to the pelvis. Thanks to this torsional movement of the upper body, the pelvis was turned sideways and thus slid off the fender. On the other hand, the Žilina dummy does not allow for such movements as a rigid body. Figure 18 displays the throw distance chart for complete hits and in-crash braking, and figure 19 depicts the throw distance chart for partial hits.

It can be concluded that both the biofidelic and Žilina dummy "produce" expected throw distances. However, as the throw distance charts have been developed partially based on crash tests with the Žilina dummy, the charts are slightly biased towards the Žilina dummy. Nonetheless, the results from the biofidelic dummy are very pleasing and further corroborate the validity of the throw distance charts.

"Dummy injuries"

"Autopsies" of the eight biofidelic dummies have been conducted at the "Bureau for Accident Reconstruction Berlin".

The damages of the biofidelic dummies have been determined by dismembering the ATDs and these damages have then been translated into respective injuries of a human being. It must be noted, however, that only bone fractures have been analysed, as the biofidelic dummy cannot mimic injuries to tissues and organs.

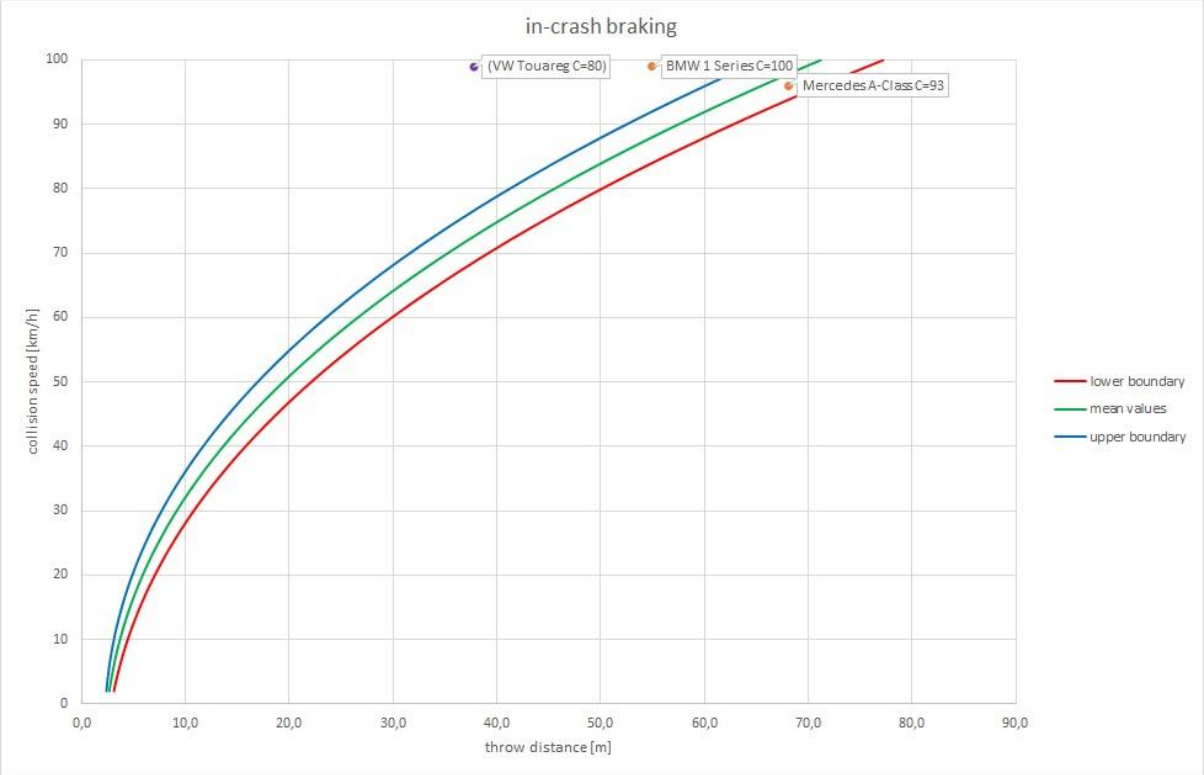

Figure 18. Throw distance chart for complete hits and in-crash braking.

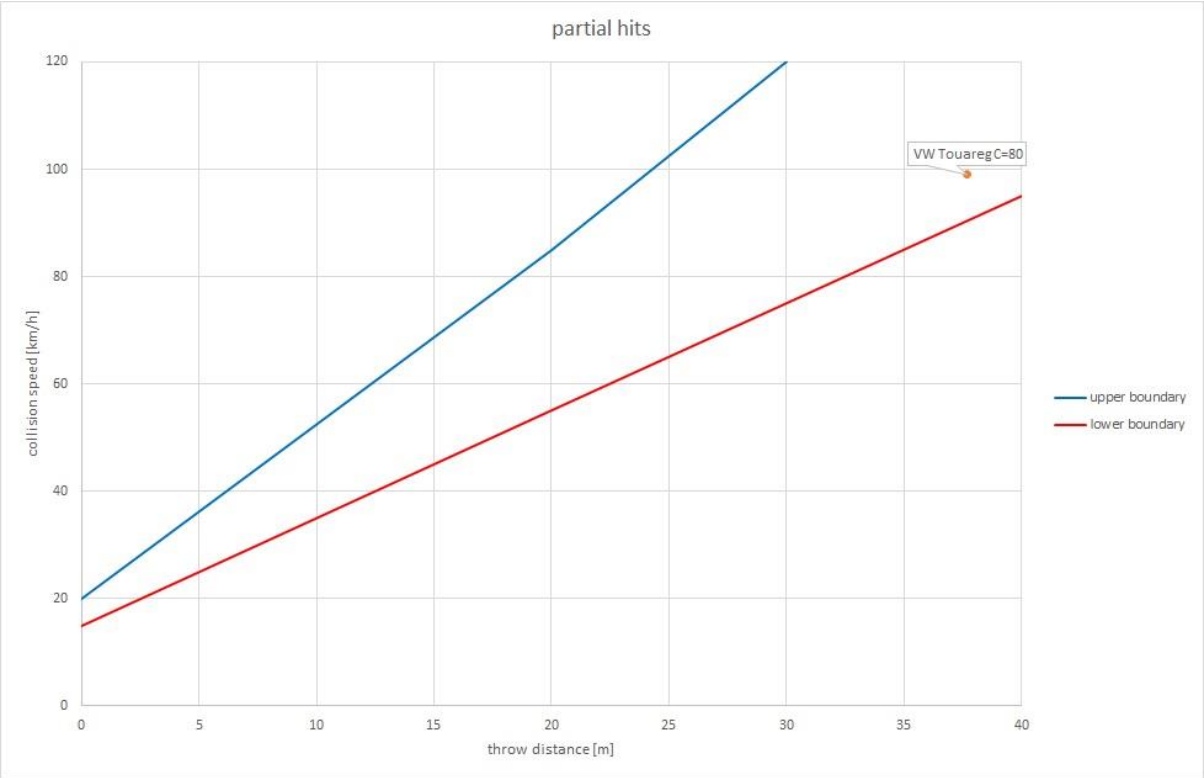

Figure 19. Throw distance chart for partial hits.

In [5], one of the authors analysed the correlations between collision parameters, vehicle damages and pedestrian injuries and concluded that the fracture patterns of long bone fractures in the lower limbs, knee joint injuries, injuries to the ankle, pelvic injuries and head injuries can be used for reconstruction purposes. The following analysis of the biofidelic dummy's "injuries" therefore focuses on these injuries, because the main area of use of this ATD will be in accident reconstruction. Figure 20 shows an overview of the "autopsy" of the biofidelic dummy used in crash test wh18.25.

Figure 20. Overview of the "autopsy" of the biofidelic dummy used in crash test wh18.25.

Fracture patterns of the lower leg's long bones The characteristic wedge-shaped fracture pattern, known as the Messerer's wedge fracture, can be often found in pedestrians hit by a vehicle [6]. The apex points in the direction of the vehicle's velocity vector and is thus indicative of the direction of impact.

While the fracture of the biofidelic dummy's lower leg does not exhibit the characteristic two faces of the Messerer's wedge fracture with the apex showing in the impact direction, a unique fracture pattern can be still observed. Initially, the fracture surface is flat and then ends with a protrusion on one of the two fracture surfaces. As with the apex of the Messerer's wedge fracture, this protrusion always indicates the impact direction.

Bone is a heterogeneous material, whereas the ATD's bones are made of a homogeneous material with similar strength. This difference explains the different fracture patterns observed in human beings and the biofidelic dummy. Notwithstanding, the biofidelic dummy exhibits a fracture pattern comparable to the Messerer's wedge fracture which can be used as a supporting factor in determining the impact direction. Figure 21 shows the fracture pattern observed in the biofidelic dummy used in crash test wh18.23.

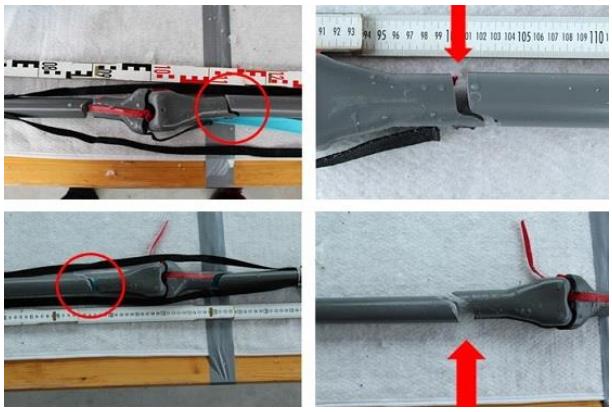

Figure 21. Messerer's wedge fracture in the biofidelic dummy used for crash test wh18.23 (Top: Left side; Bottom: Right side; Red circle: Location of wedge-shaped fracture; Red arrow: Impact direction).

Knee joint injuries The knee injuries sustained by the pedestrian can be classified according to their mechanism, namely avulsive or compressive. The resulting injuries to the condyles, the collateral ligaments and the cruciate ligaments are indicative of the impact direction. While valgus flexion was primarily found in lateral hits, varus flexion was found in medial ones.

The biofidelic dummy's knees have a very humanoid anatomy. The biofidelity of the dummy's knee joint injuries is analysed by means of the left knee joints of the ATDs used in crash tests wh18.23 and wh18.25, which are shown in figures 22 and 23. The underlying injury mechanism is varus flexion.

Figure 22. Knee injury of the biofidelic dummy used in crash test wh18.23 (Left: Front view; Right: Rear view; Red arrow: Impact direction).

Considering crash test wh18.23 and figure 22, the black tape, representing the lateral collateral ligament, has been torn off the femur. The tapes are glued to the bones. Here, the attachment site was weaker than the tape itself, which is why the tape was torn off and did not rupture. In reality, however, the ligament would rupture. Nonetheless, this damage to the biofidelic dummy's knee can be interpreted as a ruptured lateral collateral ligament. Moreover, both the anterior and the posterior cruciate ligaments are frayed. These "injuries" coincide with those found by [7] in human beings.

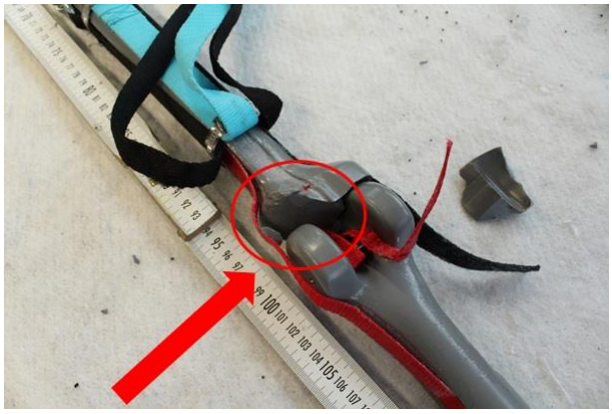

Figure 23. Rear view of the knee injury of the biofidelic dummy used in crash test wh18.25 (Red circle: Location of medial tibial condyle fracture; Red arrow: Impact direction).

Considering crash test wh18.25 and figure 23, the induced bending was even stronger, resulting in the fracture of the medial tibial condyle. In addition, the lateral collateral ligament as well as both the anterior and posterior cruciate ligaments were ruptured. The medial collateral ligament was also frayed by the impact.

Injuries to the ankle The "injuries" to the biofidelic dummy's ankle cannot be analysed as of yet, as the ankle's anatomy is not humanoid at all. The foot, made of rubber, is simply screwed into the lower leg.

Pelvic injuries Pelvis injuries seem to be more common in pedestrians, who have been run over, than in those hit close to an upright posture.

[8] determined that injuries to the sacroiliac joint were the best parameter to determine the side of impact in case of lateral hits, and were found to occur, with very few exceptions, on the side of direct impact.

Of the eight biofidelic dummies tested, only those used in crash tests wh18.24 and wh18.26 exhibited fractures of the right sacroiliac joint, while those used in crash tests wh18.28 and wh18.29 exhibited fractures of the left sacroiliac joint. Figure 24 displays the fractures of the right sacroiliac joint, whereas figure 25 displays the fractures of the left sacroiliac joint.

Figure 24. Fracture of the right sacroiliac joint of the biofidelic dummy (Left: Crash test wh18.24; Right: Crash test wh18.26; Red circle: Location of fracture; Red arrow: Impact direction).

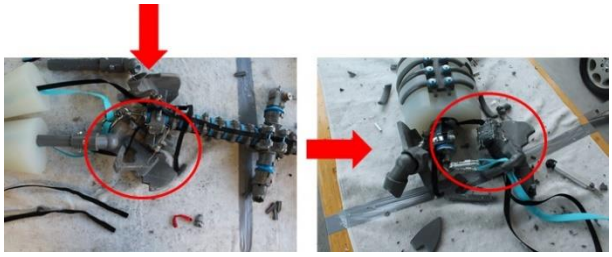

Figure 25. Fracture of the left sacroiliac joint of the biofidelic dummy (Left: Crash test wh18.28; Right: Crash test wh18.29; Red circle: Location of fracture; Red arrow: Impact direction).

The "injuries" to the sacroiliac joint found are in concordance with those reported by [8]. However, only two "injuries" occurred at the direct side of impact, while the other two occurred at the opposite side of impact.

The biofidelic dummies used in crash tests wh18.25 and wh18.27 sustained "injuries" to the ilium very close to the sacroiliac joint. Both biofidelic dummies sustained a fracture to the right ilium. As these "injuries" are so close to the sacroiliac joint, they could be considered as sacroiliac injuries for reconstruction purposes. The fractures of the left and right ilium of the biofidelic dummy used in crash test wh18.23 are further away from the respective sacroiliac joints and can hence hardly be considered as "injuries" to the sacroiliac joint region. This classification, of course, is somewhat subjective. Obviously, the design of the biofidelic dummy and the way it is constructed influence the "injury" patterns. Figure 26 shows the fracture to the ilium within the sacroiliac joint region, while figure 27 shows the fracture to the ilium outside the sacroiliac joint region.

Figure 26. Fracture of the ilium next to the sacroiliac joint of the biofidelic dummy (Left: Crash test wh18.25; Right: Crash test wh18.27; Red circle: Location of fracture; Red arrow: Impact direction).

Thus, of the six "injuries" to the sacroiliac joint region, four occurred at the direct side of impact and two at the opposite side of impact. Though the sample size is too small to make a valid statement, these findings suggest that injuries to the pelvic region are less reliable for reconstruction purposes than those to the knee joint for example.

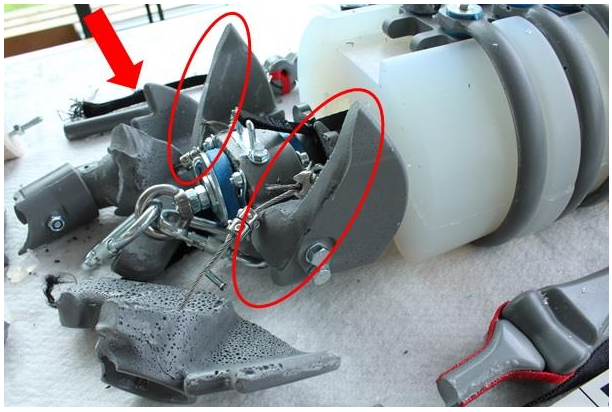

Figure 27. Fracture of the left and right ilium of the biofidelic dummy used in crash test wh18.23 (Red circle: Location of fracture; Red arrow: Impact direction).

"Injuries" to the biofidelic dummy's acetabulum were also frequently noted. According to [8], these injuries, however, are less useful for reconstruction purposes. Nonetheless, the damages of the biofidelic dummies' acetabulums are largely in concordance with the injury mechanism as described by [8]. However, bony split-offs have also been noted at the left acetabulum, i.e. the opposite side of impact.

All in all, the "injuries" to the pelvic region seem to be pretty realistic and are largely in concordance with those reported in literature. Still, many "injuries" were found on the left side of the biofidelic dummy. According to [8], though, pelvic injuries rather occur on the direct side of impact, i.e. the right side of the biofidelic dummy. In how far the design and the construction of the biofidelic dummy's pelvis influence the injury patterns requires further investigation. While many tendons and ligaments support the human pelvic region, the ATD's pelvic region is not supported.

Head injuries As with injuries to the ankle, head injuries cannot be analysed as of yet. This is due to the rigid design of the head. The latest design consists of one cast component with a cavity at the base of the skull. Inside of this rectangular cavity sits the mount of the spinal column. As this mount is more or less a rigid rectangular block, it props up the skull. Thus, the overall design of the cranium is so rigid that it does not break.

One example is the biofidelic dummy used in crash test wh18.25. Here, the ATD was hit at 99 km/h and the head impacted the A-pillar. The only "injuries" the ATD sustained to the head can be described as a laceration of the latex/wet suit with abrasions on the os parietale beneath. In reality, the skull would have fractured, resulting in severe injuries to the brain which would not have been survivable with an extreme likelihood.

Comparison with real-world pedestrian accidents As with the vehicle damages, crash tests wh18.22 and wh18.26 are compared with two real-world pedestrian accidents. The considered accidents are the same.

Without comparing every single injury, it can be noted that overall the injuries of the biofidelic dummy match those of the pedestrians pretty well. Both the pedestrians as well as the biofidelic dummies suffered injuries to the thorax, shoulder region, pelvic region, and the lower extremities.

Obviously, one must consider that the pedestrians and ATDs each collided with different vehicles. Furthermore, the individual fitness of a human being also affects their biomechanical response, explaining variations in the injury patterns. The exact kinematics and dynamics throughout the collision further influence the biomechanics and a crash test will never be able to exactly imitate those.

Nonetheless, it can be concluded that the biofidelic dummy exhibits very similar injuries to pedestrians when considering fractures. As of yet, the biofidelic dummy cannot mimic tissue and organ injuries. Figure 28 displays the different injury diagrams.

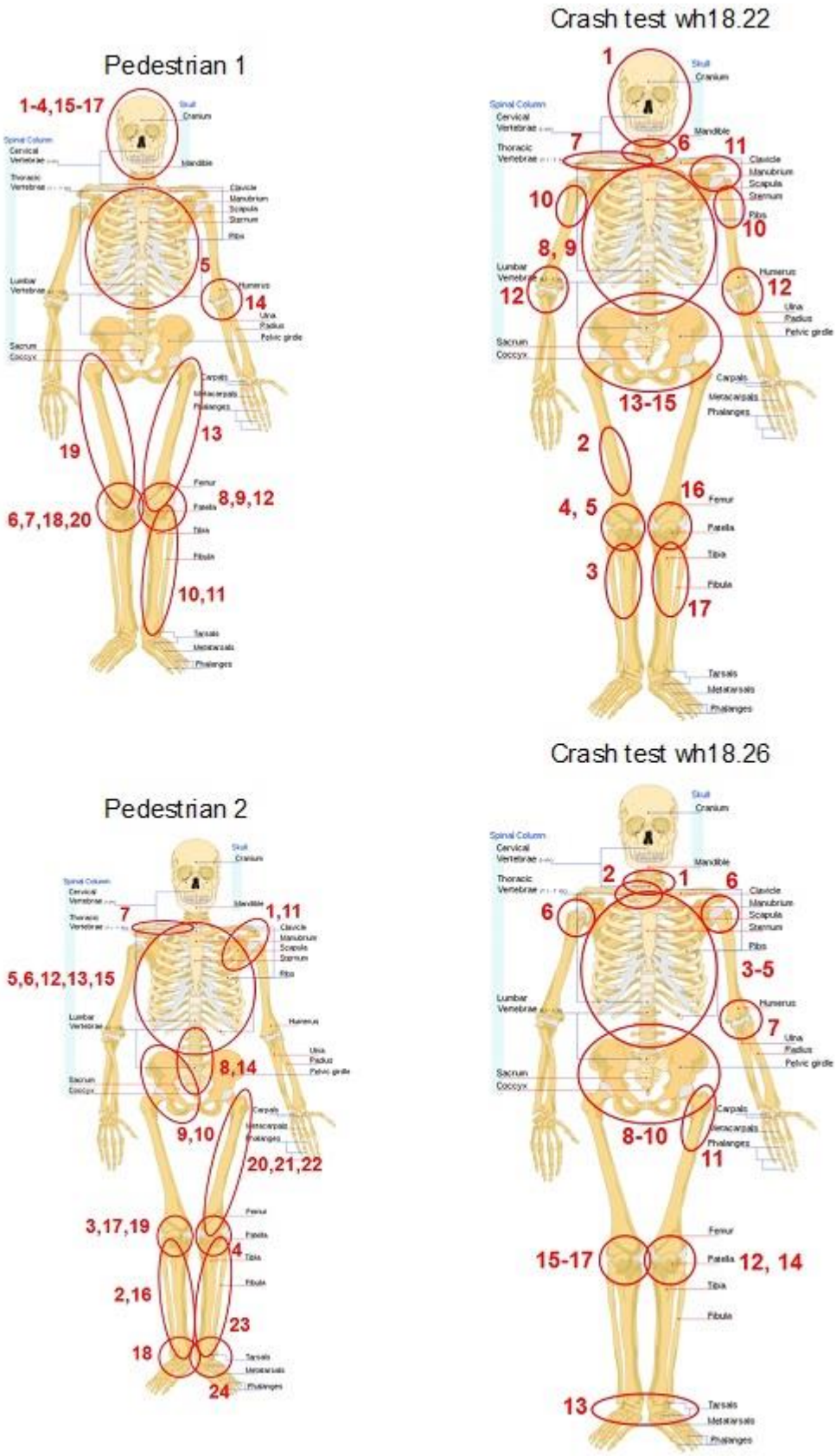

Figure 28. Comparison of injuries between pedestrian and biofidelic dummy.

LIMITATIONS

While the representational crash tests conducted by DEKRA and AXA Insurance with the biofidelic dummy were performed at roughly 70 km/h and 100 km/h, the Žilina dummy and cadaver tests had been conducted at roughly 40 km/h. This makes a direct comparison somewhat complicated due to different impact energies. But former crash tests had been conducted successfully with the Žilina dummy as well as the biofidelic dummy at impact speeds between roughly 40 km/h and 75 km/h. Nonetheless, different vehicles were used, which also has an impact on dummy/cadaver dynamics and kinematics.

As the dummy targets were placed manually on the ATDs in the video analysis programme "Falcon", the determination of the trajectories and C-ratios is further afflicted with minor inaccuracies. However, each value was computed three times and the average has been taken, in order to minimize the inaccuracies as much as possible.

The biofidelic dummy can further only mimic fractures and not injuries to tissues and organs.

CONCLUSIONS

The biofidelic dummy already exhibits a high degree of biofidelity. Its trajectories are comparable with those of PMHSs and this ATD also creates realistic vehicle damages. This allows to more correctly determine the collision speed. The obtained C-ratios are also good and the deviations to those obtained by the Žilina dummy are minimal. It can be concluded that the current procedure of determining the geometrical C-ratio based on the Žilina dummy is still valid and can be further used. The method should only be revised, in order to further refine the correctness of the results. This, however, merits further investigations. The throw distances obtained with the biofidelic dummy are good. The unique feature of the biofidelic dummy is its ability to mimic injuries a pedestrian would suffer in a pedestrian-vehicle accident of similar severity. The "injuries" of the ATD resemble those of a pedestrian pretty well, especially those of the knee joint. Thus, the biofidelic dummy enables expert witnesses to reconstruct a pedestrian-vehicle accident and to obtain realistic vehicle damages, throw distances and injuries. This opens up new possibilities in the field of accident reconstruction.

As long as the mechanical loading parameters need to be determined in a certified way, however, there is no way around the sophisticated ATDs of the like of Hybrid-III dummy, THOR dummy and POLAR dummy.

REFERENCES

[1] Knape, M. 2016. "Weiterentwicklung eines biofidelen Fußgänger-Dummys zur realistischen Schadenerzeugung an Fahrzeugen bei experimentellen Simulationen von PKW/Fußgängerkollisionen". Technische Universität Berlin. (Master's thesis)

[2] Kolla, E., Korbel, T., Imrich, L., Kubjatko, T., & Mackovicová, L. 2017. "Correlation "impact velocity-specific pedestrian injuries" for reconstruction of pedestrian accidents". Proceedings of the 26th Annual Congress of the European Association for Accident Research and Analysis, 213-224.

[3] Subit, D., Kerrigan, J., Crandall, J., Fukuyama, K., Yamazaki, K., Kamiji, K., & Yasuki, T. 2008. "Pedestrian-Vehicle Interaction: Kinematics and Injury Analysis of four full-scale Tests". Proceedings of the 2008 IRCOBI Conference – Bern (Switzerland), 275-294.

[4] Kerrigan, J. R., Murphy, D. B., Drinkwater, D. C., Kam, C. Y., Bose, D. & Crandall, J. 2005. "Kinematic Corridors for PMHS tested in full-scale Pedestrian Impact Tests". University of Virginia Center for Applied Biomechanics.

[5] Schäuble, A. 2018. "Analysis of Pedestrian Accidents - Correlations between Collision Parameters, Vehicle Damages and Pedestrian Injuries". Vienna University of Technology & DEKRA. (Project report)

[6] Hartwig, S. 2016. "Personenschäden im Straßenverkehr: Unfallanalyse, Medizin und Recht. (W. H. M. Castro, M. Becke & M. Nugel, Eds.). C. H. Beck.

[7] Teresinski, G., Madro, R. 2001. "Knee joint injuries as a reconstructive factors in car-to-pedestrian accidents". Forensic Science International, 124, 74-82.

[8] Teresinski, G., Madro, R. 2001. "Pelvis and hip joint injuries as a reconstructive factors in car-to-pedestrian accidents. Forensic Science International, 124, 68-73.